



City Research Online

City, University of London Institutional Repository

Citation: Vogiatzaki, K., Kronenburg, A., Navarro-Martinez, S. & Jones, W. P. (2011). Stochastic multiple mapping conditioning for a piloted, turbulent jet diffusion flame. *Proceedings of the Combustion Institute*, 33(1), pp. 1523-1531. doi: 10.1016/j.proci.2010.06.126

This is the accepted version of the paper.

This version of the publication may differ from the final published version.

Permanent repository link: <https://openaccess.city.ac.uk/id/eprint/8105/>

Link to published version: <https://doi.org/10.1016/j.proci.2010.06.126>

Copyright: City Research Online aims to make research outputs of City, University of London available to a wider audience. Copyright and Moral Rights remain with the author(s) and/or copyright holders. URLs from City Research Online may be freely distributed and linked to.

Reuse: Copies of full items can be used for personal research or study, educational, or not-for-profit purposes without prior permission or charge. Provided that the authors, title and full bibliographic details are credited, a hyperlink and/or URL is given for the original metadata page and the content is not changed in any way.

City Research Online:

<http://openaccess.city.ac.uk/>

publications@city.ac.uk

Manuscript Number:

Title: Stochastic Multiple Mapping Conditioning for a turbulent jet diffusion flame

Article Type: Research Paper

Keywords: turbulent combustion modelling, turbulent diffusion flames, reacting flows, multiple mapping conditioning

Corresponding Author: Dr. Andreas Kronenburg,

Corresponding Author's Institution: University of Stuttgart

First Author: Konstantina Vogiatzaki

Order of Authors: Konstantina Vogiatzaki; Andreas Kronenburg; Salvador Navarro-Martinez; William P Jones

Abstract: A stochastic implementation of the Multiple Mapping Conditioning (MMC) approach has been applied to a turbulent jet diffusion flame (Sandia Flame D). This implementation combines the advantages of the basic concepts of a mapping closure methodology with a probability density approach. A single reference variable has been chosen. Its evolution is described by a Markov process and then mapped to the mixture fraction space. Scalar micro-mixing is modelled by a modified "interaction by exchange with the mean" (IEM) mixing model where the particles mix with their -in reference space- conditionally averaged means. The formulation of the closure leads to localness of mixing in mixture fraction space and consequently improved localness in composition space. Results for mixture fraction and reactive species are in good agreement with the experimental data. The MMC methodology allows for the introduction of an additional "minor dissipation time scale" that controls the fluctuations around the conditional mean. A sensitivity analysis based on the conditional temperature fluctuations as a function of this time scale does not endorse earlier estimates for its modelling, but only relatively large dissipation time scales of the order of the integral turbulence time scale yield acceptable levels of conditional fluctuations that agree with experiments. With the choice of a suitable dissipation time scale, MMC-IEM thus provides a simple mixing model that is capable of capturing extinction phenomena, and it gives improved predictions over conventional PDF predictions using simple IEM mixing models.

Stochastic Multiple Mapping Conditioning for a piloted, turbulent jet diffusion flame

K. Vogiatzaki^a, A. Kronenburg^{a,*}, S. Navarro-Martinez^b,
W.P. Jones^b

^a*Institut für Technische Verbrennung, University of Stuttgart, 70569 Stuttgart,
Germany*

^b*Department of Mechanical Engineering, Imperial College London, SW7 2AZ,
U.K.*

Colloquium: Turbulent Flames

Total length is 5741 words determined by method 2 for latex users

main text: 3359; references: 402 (method 1)

Figure 1: 462 (two column figure)

Figure 2: 165

Figure 3: 165

Figure 4: 418 (two column figure)

Figure 5: 418 (two column figure)

Figure 6: 176

Figure 7: 176

* Corresponding author: A. Kronenburg, Institut für Technische Verbrennung, University of Stuttgart, Herdweg 51, 70174 Stuttgart, Germany, Fax: +49-711-68555635
Email address: a.kronenburg@itv.uni-stuttgart.de (A. Kronenburg).

Stochastic Multiple Mapping Conditioning for a piloted, turbulent jet diffusion flame

K. Vogiatzaki^a, A. Kronenburg^{a,*}, S. Navarro-Martinez^b,
W.P. Jones^b

^a*Institut für Technische Verbrennung, University of Stuttgart, 70569 Stuttgart,
Germany*

^b*Department of Mechanical Engineering, Imperial College London, SW7 2AZ,
U.K.*

Colloquium: Turbulent Flames

Total length is 5741 words determined by method 2 for latex users

main text: 3359; references: 402 (method 1)

Figure 1: 462 (two column figure)

Figure 2: 165

Figure 3: 165

Figure 4: 418 (two column figure)

Figure 5: 418 (two column figure)

Figure 6: 176

Figure 7: 176

* Corresponding author: A. Kronenburg, Institut für Technische Verbrennung, University of Stuttgart, Herdweg 51, 70174 Stuttgart, Germany, Fax:+49-711-68555635
Email address: a.kronenburg@itv.uni-stuttgart.de (A. Kronenburg).

Abstract

A stochastic implementation of the Multiple Mapping Conditioning (MMC) approach has been applied to a turbulent jet diffusion flame (Sandia Flame D). This implementation combines the advantages of the basic concepts of a mapping closure methodology with a probability density approach. A single reference variable has been chosen. Its evolution is described by a Markov process and then mapped to the mixture fraction space. Scalar micro-mixing is modelled by a modified “interaction by exchange with the mean” (IEM) mixing model where the particles mix with their -in reference space- conditionally averaged means. The formulation of the closure leads to localness of mixing in mixture fraction space and consequently improved localness in composition space. Results for mixture fraction and reactive species are in good agreement with the experimental data. The MMC methodology allows for the introduction of an additional “minor dissipation time scale” that controls the fluctuations around the conditional mean. A sensitivity analysis based on the conditional temperature fluctuations as a function of this time scale does not endorse earlier estimates for its modelling, but only relatively large dissipation time scales of the order of the integral turbulence time scale yield acceptable levels of conditional fluctuations that agree with experiments. With the choice of a suitable dissipation time scale, MMC-IEM thus provides a simple mixing model that is capable of capturing extinction phenomena, and it gives improved predictions over conventional PDF predictions using simple IEM mixing models.

Key words: turbulent diffusion flame, modelling, scalar mixing, multiple mapping conditioning

1 Introduction

As the concern for the environment increases and more stringent legislation requires higher efficiency and reduced emissions, modern combustion systems tend to use leaner mixtures and run at lower temperatures to restrict the formation of NO_x . These facts lead to an increased interest in the modelling of flows with substantial finite rate chemistry effects and advanced combustion models that allow an accurate prediction of the interaction between chemical reaction and turbulent mixing are needed.

Probabilistic methods such as the probability density function (PDF) [1] methods have been established as powerful modelling tools for combustion processes since they allow for a direct and therefore, accurate closure of the chemical reaction rate. However, the modelling of mixing process poses two problems: Firstly, the lack of information on small scale structures and consequently lack of information on the dissipation time and secondly, the requirement for the mixing process of the stochastic particles to mimic the change in composition of the real fluid particles due to turbulent mixing. These issues lead to certain principles that should be satisfied by the mixing models such as boundedness of the scalars, linearity of scalar transport, independence of the evolution of the particle properties and -most importantly- localness in the physical and compositional spaces. Detailed discussion regarding the importance of these principles can be found in the the literature [1,2]. Here, we only emphasise the importance of localness for mixing to occur [3]. Generally improvements to the mixing model are limited by the resolution for the flow field and thus discrepancies are more pronounced in the RANS context [4]. However, results suggest that if particles mix with other particles in their immediate neighbour-

hood in composition space so that mixing across the reaction zone is avoided, the description of mixing is improved [2].

Different models have been suggested in the literature for the closure of the mixing term. Simple models that are easy to implement such as the “interaction by exchange with the mean” (IEM) [5,6] and the various Curl’s models [7,8] do not ensure localness in composition space. In the present work, we investigate the applicability of an approach that can ensure localness even if mixing is based on a simple IEM models. Multiple mapping conditioning (MMC) [9] combines the PDF method with the basic concepts of a mapping closure for the modelling of the turbulent mixing term. MMC by itself does not constitute a specific mixing model but it allows the modification of existing models so that can accommodate the principles of localness while maintaining their simplicity. The exact MMC model formulation used in the current work is introduced in the following sections. The implementation methodology and its limitations are described and predictions of the mixing field and of reactive species are compared with experimental data for a piloted methane/air jet diffusion flame (Sandia flame D) [10]. In addition, the sensitivity of the method to an additional time scale, the minor dissipation time, is tested.

2 Reference space

The basic idea of the mapping closure concept [11,12] used in the MMC methodology is to employ turbulent fluctuations and small-scale mixing in a mathematical reference space, ξ , with a known (or prescribed) PDF, to model the turbulent fluctuations and small-scale mixing in the physical composition space, whose PDF is not known in advance. A deterministic implementation

leads to mapping functions that map the reference space to the physical space and the conditional scalar dissipation appears in closed form [13,14]. In the stochastic implementation the "randomness" of species mass fraction Y_I^* of a particle is assumed to be reflected by the randomness of the reference variable ξ^* . This assumption generates three different definitions of fluctuations in the MMC context: the unconditional fluctuations ($Y_I' = Y_I - \langle Y_I \rangle$), the major fluctuations ($Y_I'' = \langle Y_I | \xi \rangle - \langle Y \rangle$) and the minor fluctuations ($Y_I''' = Y_I - \langle Y_I | \xi \rangle$). In MMC, the particle position is tracked in reference space, mixing is allowed only among particles that are close to each other in ξ -space, and this directly controls the minor fluctuations. Ideally, events that are close to each other in physical space should also be close in composition space and thus in reference space. If this is satisfied, localness of the MMC model is ensured.

One of the challenges of the method is the estimation of the "minor dissipation time", τ_{min} , that controls the minor fluctuations. The minor fluctuations exist only in the context of MMC, and the only indication for τ_{min} is that the level of the minor fluctuations should lead to an accurate level of the "physical" conditional fluctuations [15].

In a recent study by Cleary *et al.* [16], Sandia Flame D is modelled using one reference variable obtained from a -to the particle position interpolated- LES mixture fraction field. However, this approach cannot be applied to RANS. Any particle properties interpolated from RANS statistics are mean properties and do not add any information with respect to their instantaneous compositional localness. An alternative approach is described here that can be considered an extension to the work of Wandel *et al.* [17]. It is a probabilistic MMC formulation with a single reference variable that is used to enforce localness in mixture fraction space and whose evolution is described by a Markov

process. MMC allows the choice of any number of reference variables, yet for flames with low levels of local extinction, localness in mixture fraction space is normally sufficient to indicate localness in the multidimensional composition space.

We introduce the stochastic reference variable, ξ^* , which is governed for one single reference variable by the following set of stochastic differential equations (sdes)

$$d\mathbf{x}^* = \mathbf{U}(\xi^*)dt, \quad (1)$$

$$d\xi^* = A^\circ dt + b dw^* \quad (2)$$

and a Fokker-Planck equation

$$\frac{\partial \bar{\rho} P_\xi}{\partial t} + \nabla(\mathbf{U} \bar{\rho} P_\xi) + \frac{\partial A^\circ \bar{\rho} P_\xi}{\partial \xi} - \frac{\partial^2 B \bar{\rho} P_\xi}{\partial \xi^2} = 0, \quad (3)$$

where $2B = b^2$. If we assume a distribution for the reference space then the drift and diffusion coefficients of Eq. (2) can be determined from Eq. (3).

3 The model

In the current implementation Eq. (1) and Eq. (2) that account for transport in the physical and reference space respectively, are solved jointly with

$$dY_I^* = [\Omega_I^* + S_I^*]dt, \quad (4)$$

that accounts for the evolution of the composition space. Ω_I is the reaction rate and S_I^* is the mixing term. A detailed derivation of Eqs.(1)-(4) can be found in [9]

In this paper, one of the simplest models is examined for S_I^* : the IEM mixing model. The original IEM model mixes all particles within one computational cell with their unconditional means and conventional PDF computations with IEM are denoted from hereon PDF-IEM. When using the modified IEM model (MMC-IEM) the particles are mixed with their means conditioned on a certain value in reference space, $\langle Y_I | \xi \rangle$.

According to the MMC-IEM model, S_I^* is then given by

$$S_I^* = \frac{\overline{Y_I}(\xi^*) - Y_I^*}{\tau_{min}}, \quad (5)$$

with $\langle S^* | \xi^* = \xi, x^* = x \rangle = 0$ [9].

The simplicity of the IEM model is attractive for implementation, especially as a first modelling attempt that is expected to provide qualitative understanding of the stochastic implementation of the MMC method and its application to real flames. However, a good estimate of the minor dissipation time needs to be determined. As Pope [18] pointed out PDF predictions are sensitive to the velocity-to-scalar time scale ratio C_{Y_a} value that is not known a priori. Klimenko [15] suggested that the minor dissipation time should be considerably smaller than the characteristic physical dissipation time, τ_D , performing an asymptotic analysis for an homogeneous case, and Direct Numerical Simulations (DNS) for simple homogeneous flows indeed suggest $\tau_{min} \approx 1/8\tau_D$ as a suitable estimate for the minimum dissipation time [17]. However, in real

flames DNS is not an option, and it is far from being clear how to extract the correct dissipation time from RANS solutions for the flow field. Here, we report on results using three different values for τ_{min} .

For the current implementation a single ‘‘mixture fraction-like’’ reference variable is used. The term mixture-fraction like variable has the connotation that closeness in reference space guarantees closeness in mixture fraction space. For the derivation of coefficients A^o and B a Gaussian distribution of ξ^* is assumed, and the coefficients are then given in the following form [9]

$$\mathbf{U} = \mathbf{U}(\xi; \mathbf{x}, t) = \mathbf{U}^{(0)} + \mathbf{U}^{(1)}\xi, \quad (6)$$

$$A^o = -\frac{\partial B}{\partial \xi} + B\xi + \frac{1}{\langle \rho \rangle} \nabla \langle \rho \rangle \mathbf{U}^{(1)} + \frac{2}{P_\xi} \frac{\partial B P_\xi}{\partial \xi}, \quad (7)$$

$$\mathbf{U}^{(0)} = \tilde{\mathbf{v}}, \quad (8)$$

$$\mathbf{U}^{(1)} \langle \xi Z \rangle = \langle \mathbf{v}'' Z'' \rangle, \quad (9)$$

where $\tilde{\mathbf{v}}$ is the mean flow field velocity. The turbulent flux can be modelled by a standard gradient approximation ($\langle \mathbf{v}'' Z'' \rangle = -D \nabla \langle Z \rangle$). B is modelled independently of ξ , ($B = B(\mathbf{x}, t)$) [9], and is related to scalar dissipation $\langle N_Z \rangle$ by

$$B \left\langle \left(\frac{\partial Z}{\partial \xi} \right)^2 \right\rangle = \langle N_Z \rangle. \quad (10)$$

In addition, the derivative $\partial Z / \partial \xi$ is approximated by $\partial \bar{Z} / \partial \xi$.

It is apparent from Eq. (10) that closure of the MMC model requires knowledge of the unconditional scalar dissipation of Z . The parameter $\langle N_Z \rangle$ can be modelled adopting Corrsin’s suggestion [19] that the decay rate of a passive scalar variance is assumed to be proportional to the decay rate of the turbulent

kinetic energy i.e.

$$\langle N_Z \rangle = \frac{\langle Z'^2 \rangle}{\tau_D}, \quad (11)$$

where τ_D is proportional to the flow turbulent time scale $\tau = k/\varepsilon$ with proportionality constant commonly assumed to be $C_D = 1$.

It might appear as a paradox that a distribution is assumed for a variable that in reality is solved. Equation (2), however, is solved such that every particle has its own stochastic value of ξ^* that is indicative of the distance of -say- two particles in mixture fraction space. Attributing a random value for ξ^* to every particle that is derived from a Gaussian distribution, without solving Eq. (2) might present itself as an alternative that would maintain the Gaussianity of the reference space, however, it would not offer any extra information with respect to the distance of particles in mixture fraction space. Instead, using the specific model for A^o and B introduces links between the physical space and the reference space through $U(\xi)$, $\langle N_Z \rangle$ and $\langle Z\xi \rangle$.

4 Test case and numerical implementation

The test case (Sandia Flame D) [20,10] consists of a methane/air fuel mixture that issues from a central 7.2mm diameter nozzle surrounded by coaxial pilot flame with an outer diameter of 18.2mm. The fuel is 25% CH_4 and 75% air by volume with a stoichiometric mixture fraction of $Z_{st} = 0.351$. The jet Reynolds number is 22,400, the pilot inlet velocity is 11m/s and the velocity of the co-flowing air is 0.9m/s.

The Eulerian flow field equations are solved using an in-house RANS code

(BOFFIN). Turbulence is modeled by a standard k - ε model. A cylindrical domain extends $0.65m$ in downstream direction and $0.15m$ in radial direction and is discretised by 80 axial and 50 radial finite volume cells. For the composition field there are 800.000 Lagrangian particles corresponding to an average number of around 200 particles per cell. The evolution of the particle properties is modelled by Eqs. (1), (2) and (4). It is important to emphasise that every particle carries information on its (stochastic) velocity, species concentration and ξ . Note that the reference space is Gaussian and unbounded, but the deterministic drift term counteracts the random diffusion term and keeps particles close to the mean. Then, depending on their ξ value, the particles within each cell are ordered in the reference sample space that extends from -4 to 4 and that is divided into 40 bins. Chemistry is modelled by a reduced 15-step methane-air mechanisms [21].

Two extra equations for the mean mixture fraction and its variance are also solved in the RANS context. Conventional closure are used for these deterministic equations for $\langle Z \rangle$ and $\langle Z''^2 \rangle$. The values are used to initialise Z^* and for comparison with the stochastic solutions for the mixing field.

The mapping functions of mixture fraction and of the reactive species $\overline{Y}_I(\xi^*)$ are obtained from a binning procedure. In every Eulerian cell the sample space of the reference variable is defined and divided into a number of bins. Then the particles that are in the cell are ordered depending their ξ^* value. In each ξ -bin, $\overline{Y}_I(\xi)$ is defined by an ordinary averaging process. For the ξ -bins that are empty, values are obtained from linear interpolation. The computation of $\overline{Y}_I(\xi)$ is needed for the mixing with the conditional mean, postulated by MMC-IEM.

5 Results

Three computations with different minor dissipation times have been run and are compared with experiments and solutions from deterministic, Reynolds-averaged transport equations for mean mixture fraction and its variance. The three mixing time scales that are investigated here are $\tau_{min} = \tau_d$, $\tau_{min} = 0.7\tau_d$ and $\tau_{min} = 0.5\tau_d$.

Figure 1 shows the mixture fraction profiles over the reference space at various axial locations and $r/D = 1$ for the three test cases of the MMC-IEM mixing model. It can be seen that particles cluster around the conditional mean (solid line). At upstream locations the slope is rather moderate due to the low mixture fraction variance in these areas. Downstream the slope increases. There is significant scatter around $\bar{Z}(\xi)$ for all three cases, however there are quantitative differences. As τ_{min} decreases, mixing becomes more intense, particles are mixed faster towards their conditional means and fluctuations are reduced.

This - of course- affects predictions for mixture fraction mean and in particular its variance. Figures 2 and 3 show radial profiles of mean and rms of mixture fraction Z at different axial locations. Predictions MMC-IEM are presented and compared with experimental data. Predictions from the solution of the conventional RANS equations (solid lines) and from PDF-IEM (diamonds) are also included, but no results are shown for $\tau_{min} = 0.7\tau_d$ for clarity of presentation. Predicted mixture fractions and rms generally fall between predicted values for $\tau_{min} = \tau_d$ and $\tau_{min} = 0.5\tau_d$.

Overall the predictions are in qualitative agreement with the experimental data for all time scales. Mean mixture fraction is well predicted everywhere

in the domain and the differences are rather small between all models. With respect to mixture fraction variance, differences are more pronounced. The predictions are generally good and they constitute a slight improvement in comparison to the deterministic RANS and PDF-IEM predictions. However, the effects of different time scales are apparent and consistent with Fig.1. In Fig.3, dashed lines denote computations with $\tau_{min} = \tau_D$ and stars represent $\tau_{min} = 0.5\tau_D$. A smaller mixing time scale enhances mixing, it reduces the scatter around the conditional mean and therefore, predicted $\langle Z''^2 \rangle$ are noticeably decreased.

It is noted that MMC-IEM profiles are not smooth which can be attributed to the stochastic MMC implementation. The derivation of the drift and diffusion coefficients of Eq. (3) is based on the assumption of a normal distribution for ξ^* . It is important for the accuracy of the method that the computed PDFs remain close to the presumed distribution throughout the simulation. For all three test cases the agreement with the normal distribution is satisfactory (not shown), but 200 particles per cell do certainly not reproduce the exact continuous Gaussian distribution. Further, computation of $\langle Y_I^* | \xi^* = \xi \rangle$ introduces inaccuracies. The conditional mean $\langle Y_I^* | \xi^* = \xi \rangle$ is calculated for every ξ bin and therefore the calculation is based on a considerably smaller number of particles than present in the corresponding RANS cell. Temporal averaging may alleviate these problems but this is not attempted here.

The mixing model performance is now evaluated in terms of scatter plots of mixture fraction and reactive species. This is presented in Figs 4 and 5 for the MMC-IEM model. The column to the left shows the experimental data, the three columns in the middle show MMC-IEM for the three different time scales and the column to the right show “conventional” PDF-IEM computa-

tions. The agreement with experimental data in terms of conditional species profiles and peak values is rather satisfying. The degree of scattering around stoichiometric, however, is somewhat underpredicted for all time scales and our model does not seem to predict local extinction that is evident in the experiments very accurately. However, the effects of τ_{min} are evident. Only a minimum dissipation time scale of the order of the integral turbulent time scale allows some deviation from a fully burning flamelet regimes. Stronger mixing in conditional (reference) space inhibits all significant deviations from the conditional mean and reduces the degree of extinction. Small time scales of the order of $0.1\tau_D$ as suggested by [15,17], would significantly overpredict conditional mixing in Sandia Flame D, and MMC-IEM would yield very similar prediction as PDF-IEM where conditional mixing is not explicitly modelled. It can be seen in the right column that PDF-IEM predictions do not exhibit much scatter around the conditional mean which is consistent with results reported in the literature[4]. MMC-IEM is thus distinctly different from PDF-IEM that tends to destroy all conditional fluctuations, but a suitable estimate of τ_{min} should be larger than $\tau_{min} = 0.5\tau_D$. Estimates of $\tau_{min} \in 0.7\tau_D, 1.0\tau_D$ seem consistent with experiments. An increase of the minimum dissipation time scale above $\tau_{min} = \tau_D$ does not seem physical and cannot be justified. Not surprisingly, additional computations (results not shown here) have given a considerable overprediction of the mixture fraction fluctuations that cannot be consolidated with the experimental data.

A better quantitative estimate is given in Figs 6 and 7 where temperatures and their RMS are conditionally averaged on mixture fraction and plotted for different downstream positions. MMC-IEM and PDF-IEM give good predictions for the conditional temperatures. They are slightly overpredicted due to the underprediction of local extinction that could be observed in Figs. 4

and 5. Small differences can be seen for the conditional mean at $x/D = 15$ where MMC-IEM with $\tau_{min} = \tau_D$ gives somewhat lower temperature prediction due to the decreased mixing, the increased scatter and therefore increase local extinction. Differences are more pronounced in Fig.7. It is apparent that PDF-IEM and MMC-IEM with a small minimum dissipation time scale does not allow for the correct level of conditional fluctuations and the mixing implicitly oppresses variations in conditional temperature. Longer time scales yield a relatively accurate level of conditional fluctuations, in particular at $x/D = 15$ and possibly $x/D = 30$. It is not yet quite clear why conditional fluctuations remain relatively low at $x/D = 7.5$, but improvements to conventional mixing models are clear.

6 Conclusion

The current work is one of the first implementations of stochastic MMC coupled to a RANS solver for the computation of mixing and reaction in a turbulent jet flame. A single Markovian reference variable with Gaussian distribution is selected and mapped to the mixture fraction space. The advantage of the method is that despite the use of a very simple mixing model such as IEM, the localness in composition space can be enforced and the conditional fluctuations can be modelled more accurately and be better controlled. MMC can capture parts of the physical behaviour of moderately complex phenomena such as extinction and ignition and can provide accurate levels of fluctuations if a suitable estimate of τ_{min} is found. It has been shown that for a turbulent jet flame such as Sandia Flame D, the appropriate time scale needs to be close to the integral turbulence time scale and good predictions of all quantities of interest such as unconditional and conditional means of passive and reactive

scalars and their fluctuations can be achieved. Further studies, however, would need to establish the dependence of τ_{min} on Reynolds number and/or flow geometries.

7 Acknowledgments

The authors would like to thank Dr M.J. Cleary for many helpful discussions. SNM acknowledges the financial support by The Royal Society.

References

- [1] S. Pope, *Prog. Energy Combust. Sci.* 11 (2) (1985) 119 – 192.
- [2] S. Subramaniam, S. Pope, *Combust. Flame* 115 (4) (1998) 487–514.
- [3] A. Norris, S. Pope, *Combust. Flame* 83 (1-2) (1991) 27–42.
- [4] S. Mitarai, J. Riley, G. Kosly, *Phys. Fluids* 17 (4) (2005) 047101 – 1–047101–15.
- [5] C. Dopazo, *Phys. Fluids* 22 (1) (1979) 20–39.
- [6] E. O’Brien, *Turbulent Reacting Flows*, Springer-Verlang, 1980.
- [7] R. Curl, *AIChE Journal* 9 (1963) 175–181.
- [8] J. Janicka, W. Kolbe, W. Kollmann, *J. Non-Equilib. Thermodyn.* 4 (1) (1979) 47 – 66.
- [9] A. Klimenko, S. Pope, *Phys. Fluids* 15 (7) (2003) 1907–1925.
- [10] R. Barlow, J. Frank, *Piloted methane/air flames C, D, E, and F - Release 2.0*, Tech. rep., Sandia National Laboratories (2003).
- [11] A. Chen, S. Chen, R. Kraichnan, *Phys. Rev. Lett.* 63.

- [12] S. Pope, *Theor. Comput. Fluid Dyn.* 2 (5-6) (1991) 255–270.
- [13] A. Kronenburg, M. Cleary, *Combust. Flame* 155 (1-2) (2008) 215–231.
- [14] K. Vogiatzaki, M. Cleary, A. Kronenburg, J. Kent, *Phys. Fluids* 21 (2).
- [15] A. Klimenko, *Combust. Flame* 143 (4) (2005) 369–385.
- [16] M. Cleary, A. Klimenko, *Flow Turb. Comb.* 82 (4) (2008) 477–491.
- [17] A. Wandel, A. Klimenko, *Phys. Fluids* 17 (12).
- [18] S. Pope, *Proceedings of the Sixth International Workshop on Turbulent Non-Premixed Flames*.
- [19] S. Corrsin, *J. Aeronaut. Sci.* 18 (1951) 417.
- [20] R. Barlow, J. Frank, A. Karpetis, J.-Y. Chen, *Combustion and Flame* 143 (4) (2005) 433 – 449.
- [21] J. Sung, C. Law, J.-Y. Chen, *Combustion and Flame* 125 (2001) 906 – 919.

8 Figures

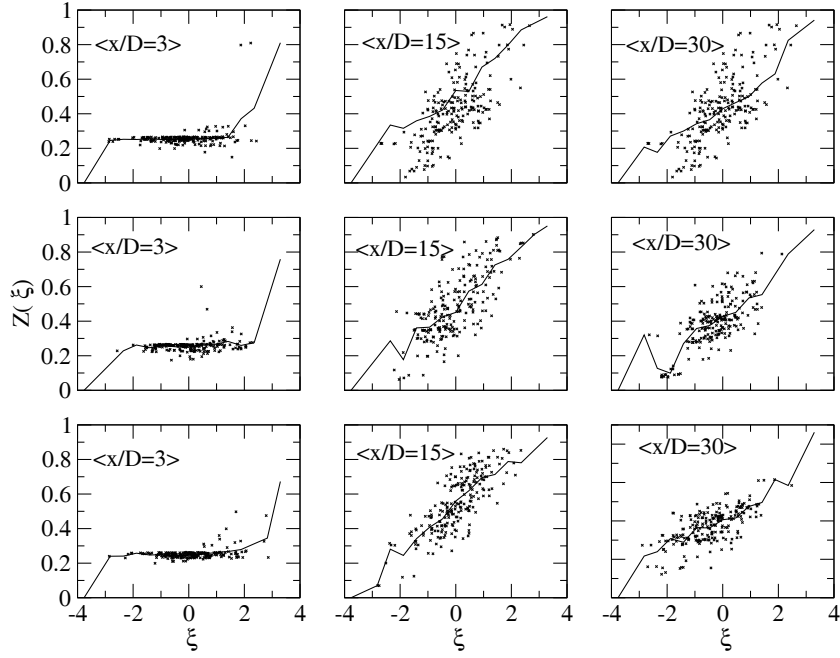


Fig. 1. Profiles of the mixture fraction in reference space at various axial locations and $r/D = 1$ for $\tau_{min} = \tau_d$ (top row), $\tau_{min} = 0.7\tau_d$ (middle row) and $\tau_{min} = 0.5\tau_d$ (bottom row). Solid lines are the profiles of $\bar{Z}(\xi)$ and symbols represent the particles.

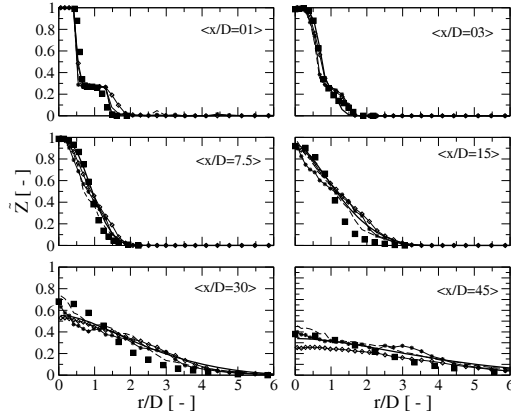


Fig. 2. Radial profiles of mean mixture fraction at different axial locations. Squares represent the experimental data, solid lines the predictions from conventional RANS equations, dashed lines the predictions from the MMC-IEM mixing model with $\tau_{min} = \tau_D$, stars the predictions from the MMC-IEM mixing model with $\tau_{min} = 0.5\tau_D$ and diamonds the predictions from PDF-IEM.

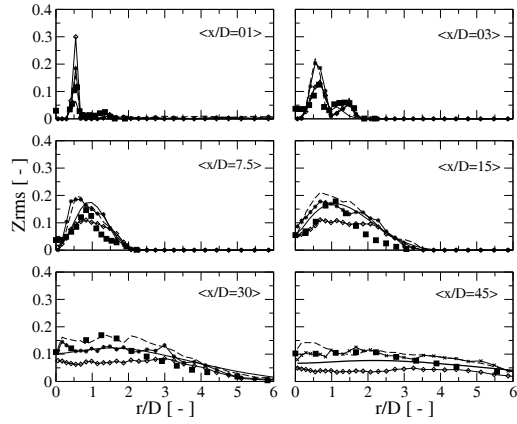


Fig. 3. Radial profiles of mixture fraction rms at different axial locations. Squares represent the experimental data, solid lines the predictions from conventional RANS equations, dashed lines the predictions from the MMC-IEM mixing model with $\tau_{min} = \tau_D$, stars the predictions from the MMC-IEM mixing model with $\tau_{min} = 0.5\tau_D$ and diamonds the predictions from PDF-IEM.

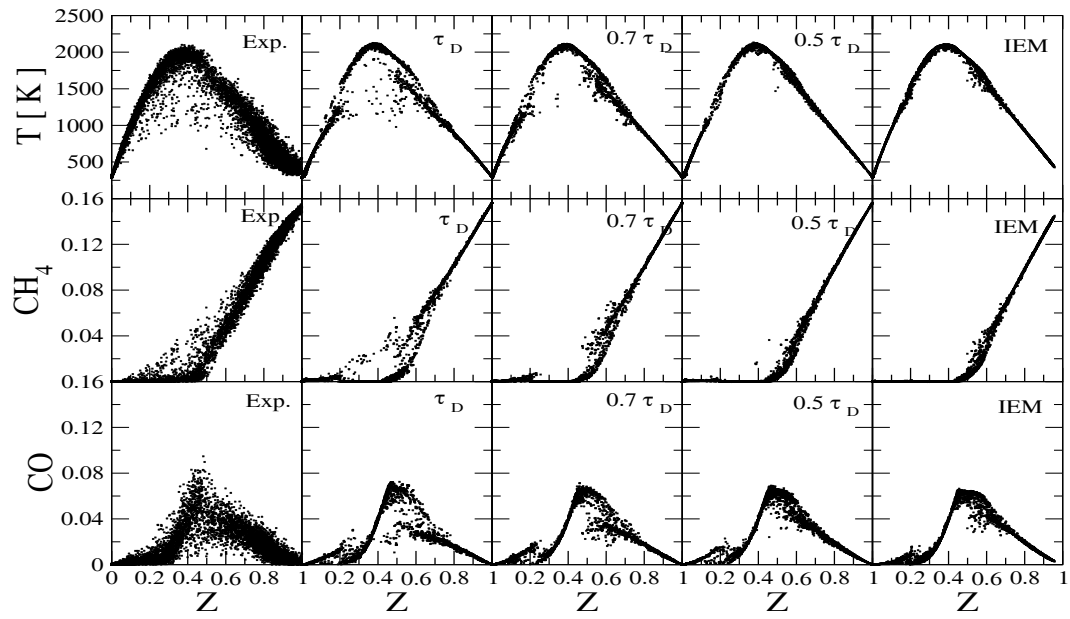


Fig. 4. Scatter plots of T, CH_4 and CO as functions of mixture fraction at $x/D = 15$.

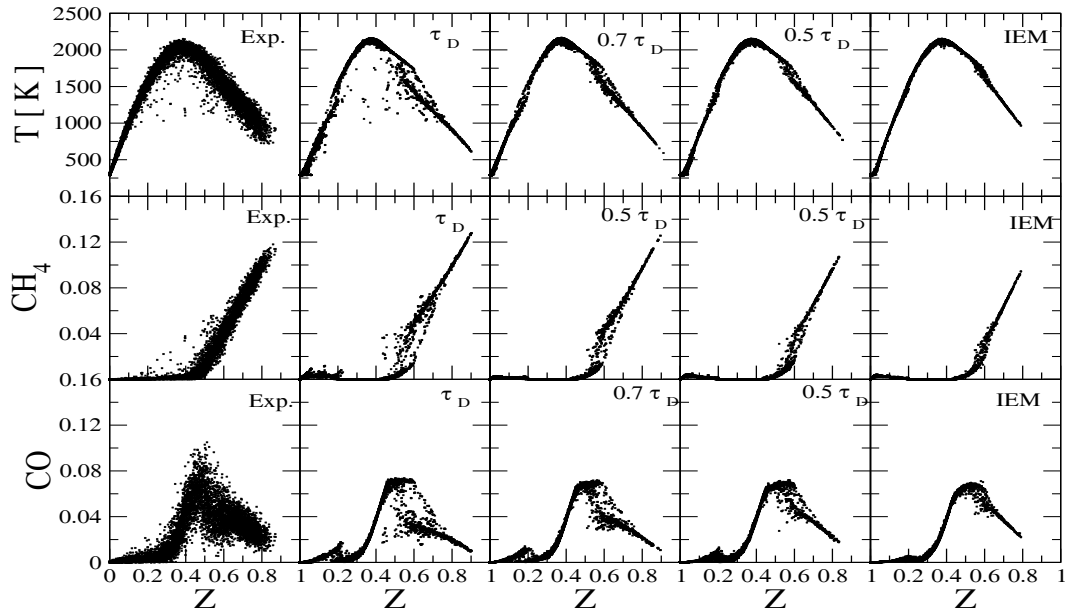


Fig. 5. Scatter plots of T , CH_4 and CO as functions of mixture fraction at $x/D = 30$.

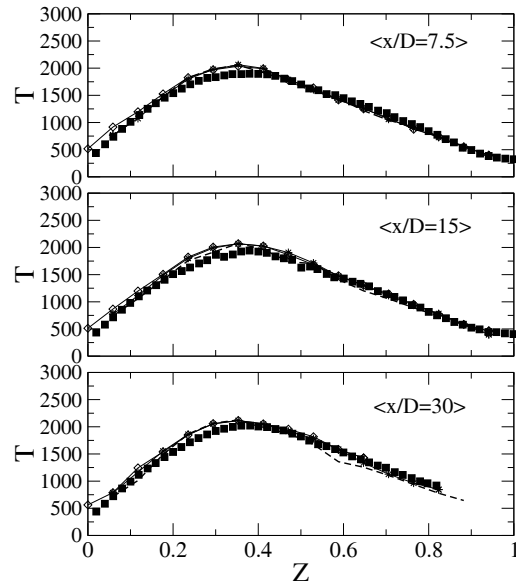


Fig. 6. Conditionally averaged temperature at different axial locations. Squares represent the experimental data, dashed lines the predictions from the MMC-IEM mixing model with $\tau_{min} = \tau_D$, stars the predictions from the MMC-IEM mixing model with $\tau_{min} = 0.5\tau_D$ and diamonds the predictions from the PDF-IEM simulations.

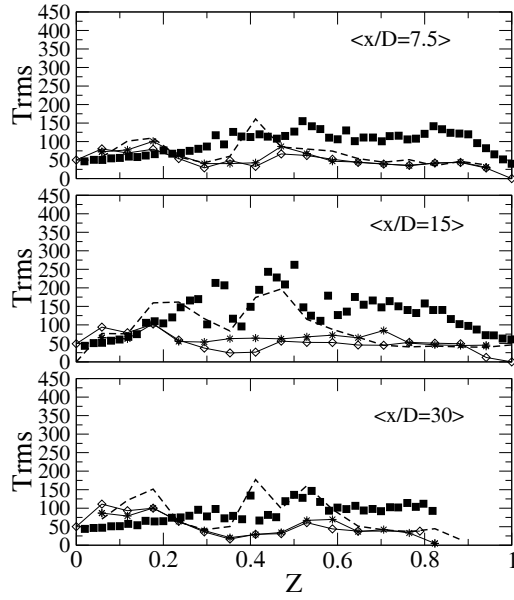


Fig. 7. Conditionally averaged temperature RMS at different axial locations. Squares represent the experimental data, dashed lines the predictions from the MMC-IEM mixing model with $\tau_{min} = \tau_D$, stars the predictions from the MMC-IEM mixing model with $\tau_{min} = 0.5\tau_D$ and diamonds the predictions from the PDF-IEM simulations.

List of Figures

- 1 Profiles of the mixture fraction in reference space at various axial locations and $r/D = 1$ for $\tau_{min} = \tau_d$ (top row), $\tau_{min} = 0.7\tau_d$ (middle row) and $\tau_{min} = 0.5\tau_d$ (bottom row). Solid lines are the profiles of $\bar{Z}(\xi)$ and symbols represent the particles. 17
- 2 Radial profiles of mean mixture fraction at different axial locations. Squares represent the experimental data, solid lines the predictions from conventional RANS equations, dashed lines the predictions from the MMC-IEM mixing model with $\tau_{min} = \tau_D$, stars the predictions from the MMC-IEM mixing model with $\tau_{min} = 0.5\tau_D$ and diamonds the predictions from PDF-IEM. 17
- 3 Radial profiles of mixture fraction rms at different axial locations. Squares represent the experimental data, solid lines the predictions from conventional RANS equations, dashed lines the predictions from the MMC-IEM mixing model with $\tau_{min} = \tau_D$, stars the predictions from the MMC-IEM mixing model with $\tau_{min} = 0.5\tau_D$ and diamonds the predictions from PDF-IEM. 18
- 4 Scatter plots of T, CH₄ and CO as functions of mixture fraction at $x/D = 15$. 18
- 5 Scatter plots of T, CH₄ and CO as functions of mixture fraction at $x/D = 30$. 19

6 Conditionally averaged temperature at different axial locations. Squares represent the experimental data, dashed lines the predictions from the MMC-IEM mixing model with $\tau_{min} = \tau_D$, stars the predictions from the MMC-IEM mixing model with $\tau_{min} = 0.5\tau_D$ and diamonds the predictions from the PDF-IEM simulations. 19

7 Conditionally averaged temperature RMS at different axial locations. Squares represent the experimental data, dashed lines the predictions from the MMC-IEM mixing model with $\tau_{min} = \tau_D$, stars the predictions from the MMC-IEM mixing model with $\tau_{min} = 0.5\tau_D$ and diamonds the predictions from the PDF-IEM simulations. 20